



PCCP

Heterogeneous Hydrogenation of Phenylalkynes with Parahydrogen: Hyperpolarization, Reaction Selectivity, and Kinetics

Journal:	<i>Physical Chemistry Chemical Physics</i>
Manuscript ID	CP-ART-05-2019-002913.R4
Article Type:	Paper
Date Submitted by the Author:	05-Nov-2019
Complete List of Authors:	Pokochueva, Ekaterina; ITC SB RAS Kovtunov, Kirill; ITC SB RAS, Salnikov, Oleg; ITC SB RAS, Gemeinhardt, Max; Southern Illinois University, Chemistry Kovtunova, Larisa; Boreskov Institute of Catalysis Bukhtiyarov, Valerii; Boreskov Institute of Catalysis, Heterogeneous Catalysis Goodson, Boyd; Southern Illinois University, Chemistry Chekmenev, Eduard; Vanderbilt University Institute of Imaging Science, Chemistry Koptyug, Igor; ITC SB RAS,

SCHOLARONE™
Manuscripts

ARTICLE

Heterogeneous Hydrogenation of Phenylalkynes with Parahydrogen: Hyperpolarization, Reaction Selectivity, and Kinetics

Received 00th January 20xx,
Accepted 00th January 20xx

DOI: 10.1039/x0xx00000x

Ekaterina V. Pokochueva^{a,b}, Kirill V. Kovtunov^{a,b†}, Oleg G. Salnikov^{a,b}, Max E. Gemeinhardt^c, Larisa M. Kovtunova^{d,b}, Valerii I. Bukhtiyarov^d, Eduard Y. Chekmenev^{e,f}, Boyd M. Goodson^{c,g†} and Igor V. Koptiyug^{a,b}

Parahydrogen-induced polarization (PHIP) is a powerful technique for studying hydrogenation reactions in gas and liquid phases. Pairwise addition of parahydrogen to the hydrogenation substrate imparts nuclear spin order to reaction products, manifested as enhanced ¹H NMR signals from the nascent proton sites. Nanoscale metal catalysts immobilized on supports comprise a promising class of catalysts for producing PHIP effects; however, on such catalysts the percentage of substrates undergoing the pairwise addition route—a necessary condition for observing PHIP—is usually low. In this paper, we present a systematic study of several metal catalysts (Rh, Pt, Pd, and Ir) supported on TiO₂ in liquid-phase hydrogenation of different prototypical phenylalkynes (phenylacetylene, 1-phenyl-1-propyne, and 3-phenyl-1-propyne) with parahydrogen. Catalyst activity and selectivity were found to be affected by both the nature of the active metal and the percentage of metal loading. It was demonstrated that the optimal catalyst for production of hyperpolarized products is Rh/TiO₂ with 4 wt% metal loading, whereas Pd/TiO₂ provided the greatest selectivity for semihydrogenation of phenylalkynes. In a study of liquid-phase hydrogenation reaction kinetics, it was shown that reaction order with respect to hydrogen is nearly the same for pairwise and non-pairwise H₂ addition—consistent with a similar nature of the catalytically active sites for these reaction pathways.

Introduction

Nowadays the development of hydrogenation catalysts that would combine both high activity and selectivity is highly desirable. In industrial processes, heterogeneous hydrogenation catalysts are often subject to high-temperature and high H₂ pressure reaction conditions;¹ thus the catalysts must be robust and recyclable for both economic efficiency and reduced environmental impact. Owing to their thermal stability, synthetic versatility, and desirable interactions with metal catalysts, the usage of titanium dioxide (TiO₂) particles as immobilizing support has received considerable attention in

recent years.² The Pd/TiO₂ catalyst has also demonstrated selectivity for specific products under different reaction conditions in a controllable manner.³ Another study investigated the chemoselectivity of Pt/TiO₂ and Pt/CeO₂ catalysts in crotonaldehyde hydrogenation, both with and without their respective supports; the results demonstrated that based on the way the catalyst and support were prepared together (support layer deposited on catalyst versus catalyst immobilized on support), the chemoselectivity toward C=C versus C=O bonds could be tuned.⁴ In the terms of liquid phase heterogeneous hydrogenation supported Pd on alumina catalysts were used for diphenylacetylene semihydrogenation.⁵ A decrease in the specific surface area along with increase in the selectivity was observed. The use of supported to MOF Ru catalysts at the mild conditions can successfully hydrogenate furfural to furfuryl alcohol.⁶ Liquid phase hydrogenation of phenylacetylene over Pd/TiO₂ was also examined in strong metal-support interaction (SMSI) regime.⁷ It is well known, that selective hydrogenation of alkynes is a big issue for industrial and academic points of view. Therefore, liquid phase hydrogenation of different alkynes was studied, where Pd catalysts were commonly used.^{8–11}

In view of all the examples provided above, examination of hydrogenation catalysts—as well as mechanisms of hydrogenation reactions—remains a highly important task.

^a International Tomography Center SB RAS, 3A Institutskaya St., 630090 Novosibirsk, Russia

^b Novosibirsk State University, 2 Pirogova St., 630090 Novosibirsk, Russia

^c Department of Chemistry and Biochemistry, Southern Illinois University, Carbondale, IL 62901, United States

^d Borekov Institute of Catalysis SB RAS, 5 Acad. Lavrentiev Pr., 630090 Novosibirsk, Russia

^e Department of Chemistry, Integrative Biosciences (Ibio), Wayne State University, Karmanos Cancer Institute (KCI), Detroit, Michigan 48202, United States

^f Russian Academy of Sciences, 14 Leninskiy Pr., 119991 Moscow, Russia

^g Materials Technology Center, Southern Illinois University, Carbondale, IL 62901, United States

†Corresponding authors, e-mail: kovtunov@tomo.nsc.ru, bgoodson@chem.siu.edu
Electronic Supplementary Information (ESI) available: [detailed preparation procedure, catalyst characterization, additional figures and experiments]. See DOI: 10.1039/x0xx00000x

NMR spectroscopy has proven to be one of the most powerful methods for such efforts; indeed, it is widely used in catalysis for characterization of homogeneous and heterogeneous catalysts, reactants and products in different phases, reaction intermediates, and more (see for example, Refs. ^{12–15}). However, one of the major disadvantages of conventional NMR is its low detection sensitivity, which results from weak nuclear spin polarization under typical thermal equilibrium conditions. In order to overcome this sensitivity problem, several hyperpolarization techniques have been developed,^{16,17} including parahydrogen-induced polarization (PHIP).^{18–20} PHIP effects can be observed via NMR during hydrogenation of unsaturated molecules with parahydrogen, provided that the hydrogenation process occurs via pairwise addition of hydrogen atoms (and the nascent H positions become magnetically inequivalent). In other words, two hydrogen atoms from one parahydrogen molecule should be added to the same reactant molecule; if this condition of pairwise addition is satisfied, NMR signals of hydrogenation products and intermediates can be significantly enhanced and exhibit characteristic antiphase lineshapes.²¹ This property has made PHIP a unique tool for mechanistic investigation of catalytic reactions, due to the possibility of sensitive intermediates detection and ability to track hydrogen atoms from the same hydrogen molecule.^{22–24}

Heterogeneous hydrogenation with parahydrogen has mostly been studied in the gas phase^{18,25–28}; however, there are examples of successful use of PHIP effects on heterogeneous catalysts (HET-PHIP) in liquid-phase hydrogenation as well.^{29–35} Initially homogeneous catalysts were utilized in the liquid phase, since in such catalysts the active site for hydrogen activation is usually a single metal center; therefore, the pairwise addition route is usually the main mechanism of hydrogenation.³⁶ On the other hand, homogeneous catalysts cannot be easily separated from hyperpolarized products, and this fact has prompted the search for other types of catalysts that can enable PHIP phenomena. One rational approach has been to immobilize homogeneous catalysts on solid supports, because ideally, such assemblies should maintain homogeneous hydrogenation mechanisms—i.e., those that favor the pairwise addition route. The first experiments of this kind were performed using Wilkinson's catalyst ($\text{RhCl}(\text{PPh}_3)_3$), supported on either modified SiO_2 or polymer particles.³⁷ Both of the resulting catalysts were able to produce PHIP signal enhancements in liquid-phase hydrogenation reactions of styrene with parahydrogen³⁷; however, later the catalysts prepared utilizing this immobilization approach were found to exhibit poor stability under reaction conditions typically necessary for hydrogenation reactions. For example, leaching of metal complexes into solution has been detected following liquid-phase hydrogenation³⁸; moreover, if the reaction is performed at high temperatures, reduction of the catalyst moieties' metal ions to form metal nanoparticles is also possible.^{39,40} These shortcomings, combined with the high cost and often tedious synthesis procedure of such catalysts, make the use of immobilized catalysts for PHIP hyperpolarization challenging on large scales.

As a result, recent efforts have been devoted to investigation of parahydrogen-induced polarization on catalysts based on metal nanoparticles — and it was previously shown that metal catalysts supported on titania usually exhibit higher selectivity to the pairwise hydrogen addition route.¹⁶ PHIP during liquid-phase hydrogenation over supported metal nanoparticles was first demonstrated in 2009 for a range of different substrates and catalysts.²⁹ It is worth noting that the work has been largely motivated by the desire to employ liquid-phase PHIP in biocompatible systems—including hydrogenation in aqueous phase.^{30,32–35} However, the main problems—low selectivity for the pairwise addition route and insufficient activity—still remain. Moreover, there is still no clear understanding of the detailed mechanism underlying the pairwise addition of hydrogen atoms on such heterogeneous (metal nanoparticle-based) catalysts.¹⁸ Therefore, in this work our goal was to perform a systematic investigation of the influence of the active metal and hydrogenation substrate on the catalytic activity and selectivity, in terms of both chemical selectivity and selectivity to pairwise addition of hydrogen.

Experimental methods

Catalyst preparation and characterization

Seven different catalysts were prepared by wet impregnation of titanium dioxide with the corresponding metal nitrates or chlorides (in case of Ir) solution: Rh/TiO₂ catalysts with 1, 4, 10, and 23 wt% metal loading, 2 wt% Pd/TiO₂, 4 wt% Ir/TiO₂, and 2 wt% Pt/TiO₂. Details of the preparation procedures can be found in the Supporting Information (SI). All catalysts were characterized by transmission electron microscopy (TEM), CO and H₂ chemisorption, and the metal loadings were determined by X-ray fluorescence on an ARL PERFORM'X analyzer with a Rh anode of an X-ray tube. Details about chemisorption procedure can be found in SI. Determined values of metal loading, dispersion, average crystallite size and mean particle size are presented in Table 1.

NMR experiments and determination of conversion and signal enhancement

Commercially available phenylacetylene (Acros Organics, 98%), 1-phenyl-1-propyne (Acros Organics, 99%), 3-phenyl-1-propyne (Acros Organics, 97%), and benzene-d₆ (Carl Roth, 99.5%) were used as received. For the PHIP experiments, hydrogen gas was enriched with parahydrogen up to 50% by passing it through a FeO(OH) powder maintained at liquid N₂ temperature. Hydrogenation experiments were performed inside a 400 MHz Bruker NMR spectrometer (i.e. the so-called PASADENA procedure²¹). Each catalyst sample (10 mg) was placed at the bottom of a 5 mm medium-walled NMR tube and 0.45 mL of a 0.1 M solution of substrate in benzene-d₆ was added. Parahydrogen ($p\text{H}_2$) was bubbled through the solution at 6.1 atm pressure for 15 s (with the following exceptions: 20 s in the case of phenylacetylene hydrogenation over 1 wt% Rh/TiO₂ and 3-phenyl-1-propyne hydrogenation over 4 wt% Pd/TiO₂; 25 s in the case of 3-phenyl-1-propyne hydrogenation over 1 wt% Rh/TiO₂). ¹H NMR spectra were acquired

ARTICLE

Table 1 Metal loading (determined by XPS), dispersion and average crystallite size (determined by CO or H₂ chemisorption), and mean particle size (determined by TEM) for all catalysts under study.

Catalyst designation	Rh ₁	Rh ₄	Rh ₁₀	Rh ₂₃	Ir ₄	Pd ₂	Pt ₂
Metal loading, wt%	1.03	3.95	9.79	23.18	4.05	1.98	2.01
Dispersion, % (CO)	84	72	30	20	45	30	46
Dispersion, % (H ₂)	95	120	49	46	93	34	42
Av. crystallite size, nm (CO)	1.3	1.6	3.7	5.5	2.2	3.7	2.5
Av. crystallite size, nm (H ₂)	1.2	0.9	2.2	2.4	1.1	3.3	2.7
Mean size (TEM), nm	0.8	1.0	1.3	2.57	0.9	2.2	1.6

immediately after termination of the gas flow using a single radio frequency (RF) pulse ($\pi/9$ tipping angle). Both conversion values (X) and PHIP signal enhancement (SE) were determined from the experiments with $p\text{H}_2$. Conversion was calculated as $X = (1 - S_{\text{aft}} / S_{\text{bef}})$, where S_{aft} is the signal intensity (integral) of the ¹H NMR signal of a given substrate (from the –CH group in the case of phenylacetylene and 3-phenyl-1-propyne, or the –CH₃ group in the case of 1-phenyl-1-propyne) after termination of hydrogen bubbling, and S_{bef} is the corresponding signal intensity before bubbling. SE was found as

$$SE = \frac{S_{\text{PHIP}} - (S_{\text{bef}} \cdot X) / 2}{S_{\text{bef}} \cdot X / n},$$

where S_{PHIP} is the intensity of the absorptive component of a given PASADENA ¹H NMR signal of the reaction product in question (from the –CH group of styrene in case of phenylacetylene hydrogenation, from the –CH group of *cis*-1-phenyl-1-propene in case of 1-phenyl-1-propyne hydrogenation, from the =CH₂ group of 3-phenyl-1-propene in case of 3-phenyl-1-propyne hydrogenation), n is the number of corresponding protons (i.e. $n=1$ for the –CH group of styrene and the –CH group of *cis*-1-phenyl-1-propene, and $n=2$ for the =CH₂ group of 3-phenyl-1-propene). In this equation $S_{\text{bef}} \cdot X$ represents the expected intensity of the NMR signal of a thermally polarized hydrogenation product (which is impossible to obtain by any other means in experiments with $p\text{H}_2$), and it should be divided by two in the numerator assuming that observed absorptive component of a PASADENA signal is the superposition of the PHIP signal and half of the thermally polarized signal (the other half of the thermal signal is superposed over the emissive part of the PASADENA signal).

Kinetics Studies.

Kinetics studies were performed with both $p\text{H}_2$ and normal hydrogen $n\text{H}_2$ (i.e., thermally-equilibrated H₂ gas with 3:1 ratio of orthohydrogen, *o*H₂, to parahydrogen, $p\text{H}_2$). For kinetics

experiments with $p\text{H}_2$, hydrogen gas was enriched with parahydrogen up to 91% by using a parahydrogen generator (Bruker BPHG 90). 10 mg of the 10 wt% Rh/TiO₂ catalyst was placed in a 5 mm medium-walled NMR tube and 0.5 mL of a 0.2 M solution of substrate (phenylacetylene, 1-phenyl-1-propyne or 3-phenyl-1-propyne) in benzene-d₆ was added. For kinetics experiments with normal hydrogen, $n\text{H}_2$ gas was bubbled through the phenylacetylene solution at 5.8 atm pressure (controlled by safety valve) for 30 seconds, and ¹H NMR spectra were acquired immediately afterwards on a 300 MHz Bruker AV 300 NMR spectrometer using a single $\pi/2$ radiofrequency pulse in a pseudo-2D mode (giving a time course comprising 512 spectra with a recording interval of 1.25 seconds). The kinetics analysis was performed using ¹H NMR signals. For kinetics experiments using parahydrogen, $p\text{H}_2$ gas was bubbled through the solution at different pressures (4.06, 2.7, or 1 atm, controlled by safety valve) for 30 seconds prior to acquisition. ¹H NMR spectra were acquired on a 300 MHz Bruker AV 300 NMR spectrometer using a single $\pi/4$ radiofrequency pulse. As above, the analysis of the kinetics data was performed using the absorptive component of the PASADENA ¹H NMR signals of reaction products.

Results and discussion

Several catalysts with different metals and metal loadings (but the same TiO₂ support material) were tested in liquid-phase hydrogenation of phenylacetylene, 1-phenyl-1-propyne, and 3-phenyl-1-propyne with parahydrogen. The catalysts showed different catalytic activity in hydrogenation of phenylacetylene, which was affected by both the nature of the active metal and the metal loading (see Figure 1; corresponding spectra for 1-phenyl-1-propyne and 3-phenyl-1-propyne hydrogenation can be found in the SI, Figures S5 and S6, respectively).

For observation of PHIP effects, two hydrogen atoms should be added to a double or triple bond in a pairwise manner, and the appearance of the antiphase signals explicitly indicates atoms originating from the same $p\text{H}_2$ molecule. As a result, in

the case of phenylacetylene hydrogenation it is possible to compare *syn* and *anti* pairwise hydrogen addition, judging by the relative intensities of hyperpolarized protons signals #3 and #4. Intensity of the signal #3 is much higher than that of the signal #4, therefore, it can be concluded that the reaction proceeds mainly via *syn* addition of parahydrogen atoms to the triple bond. As for the catalytic performance, generally rhodium catalysts displayed higher activity as well as higher selectivity to the pairwise addition, leading to more intense PHIP signals; however, catalytic behavior was found to be dependent on hydrogenation substrate as well. Calculated values of conversion rates and signal enhancements for all substrates are presented in Figure 2.

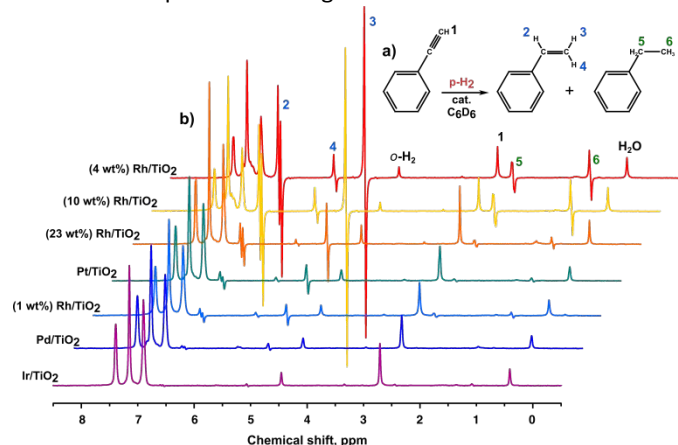


Figure 1- (a) Reaction scheme of phenylacetylene hydrogenation. (b) PASADENA ^1H NMR spectra acquired during hydrogenation of phenylacetylene with parahydrogen over different heterogeneous catalysts. Spectra are arranged (top to bottom) in descending order of PHIP.

It can be concluded that Ir/ TiO_2 is a poor choice for production of hyperpolarized products in the liquid phase, because this catalyst showed low activity in hydrogenation of all substrates and apparently sustains very little pairwise addition, since the signal enhancements were the lowest of all catalysts. On the other hand, in hydrogenation of phenylacetylene, 1-phenyl-1-propyne, and 3-phenyl-1-propyne, the largest signal enhancements were obtained with the use of 4 wt% Rh/ TiO_2 , 1 wt% Rh/ TiO_2 and 10 wt% Rh/ TiO_2 , respectively. One possible explanation of the abnormally high signal enhancement (in comparison with other catalysts) in hydrogenation of 1-phenyl-1-propyne over 1 wt% Rh/ TiO_2 , coupled with a low conversion rate, can be that the reaction is occurring in a high pairwise / low conversion regime. There are several examples of PHIP experiments^{32,41–43} in which utilized catalysts showed exceedingly high percentages of the pairwise addition (up to 11% in Ref. ⁴¹), but very low conversion (0.5% in the same work)—suggesting a similar reaction regime was present in our experiments with 1 wt% Rh/ TiO_2 .

One surprising result in the phenylacetylene reactions is that the 23 wt.% Rh/ TiO_2 catalyst appears to provide a relatively large signal enhancement, despite an anomalously low degree of reaction completion. Such a result was not observed with our previous studies with this catalyst formulation, nor was it observed with the other substrates in the present study. One

possible explanation is that in the case of alkynes (especially phenylacetylene), the strong adsorption of substrates can potentially partition the surfaces of the metal nanoparticles into smaller zones more effectively than alkenes; such smaller zones may provide more efficient pairwise $p\text{H}_2$ addition (and hence PHIP enhancement). On the other hand, we noticed that

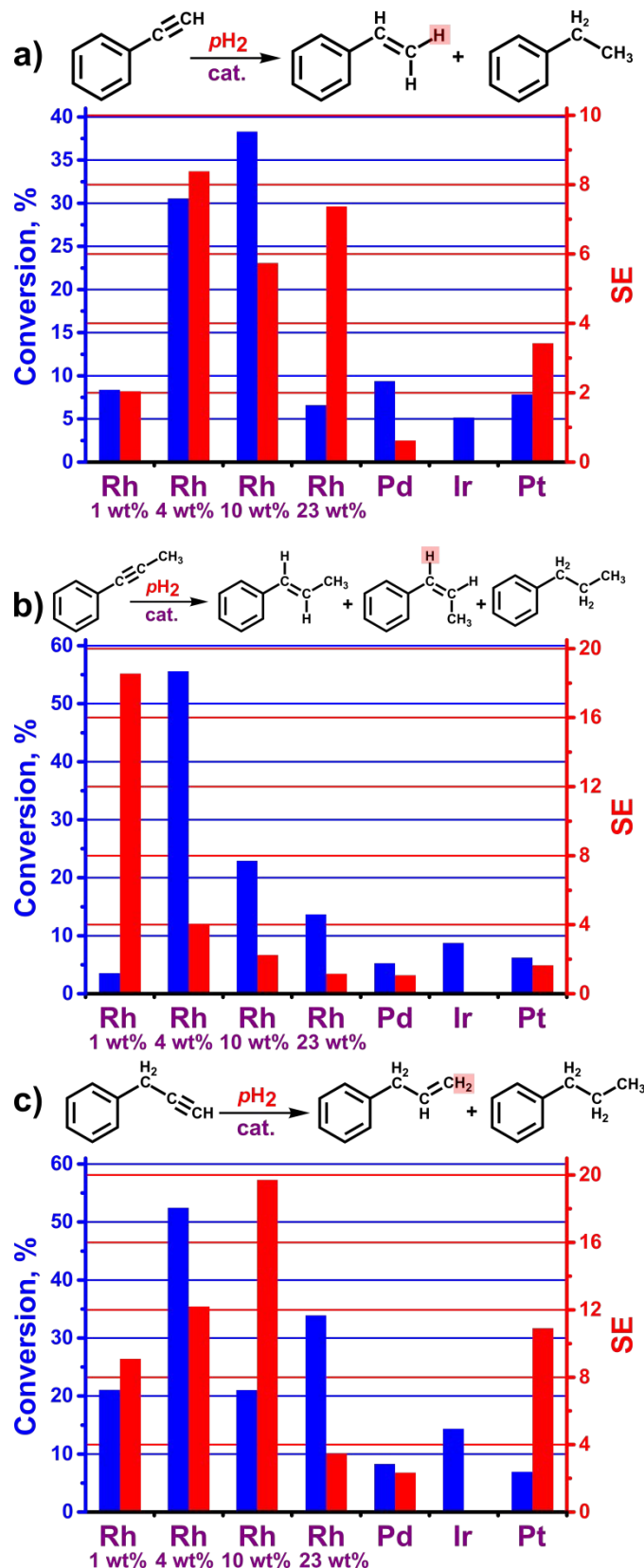


Figure 2- (a) Substrate conversion (plotted as a percentage of reaction completion over the fixed reaction time, blue) and signal enhancement (SE, red) for phenylacetylene hydrogenation over all catalysts under study. Corresponding values of conversion and signal enhancement for hydrogenation of 1-phenyl-1-propyne and 3-phenyl-1-propyne are shown in display (b) and (c), respectively.

the 23 wt% Rh/TiO₂ particles tended to more rapidly settle and lay on the bottom of the NMR tube, possibly contributing to suppressed reactivity.

Choosing between rhodium catalysts with 4 wt% and 10 wt% metal loading it is reasonable to use 4 wt% one, because it provides considerably better conversion rates. As for the rhodium catalyst with 23 wt% metal loading, it was found to be prone to sedimentation at the bottom of the NMR tube, which consequently reduces the reaction efficiency and hampering hydrogenation.

It should be noted that during hydrogenation, the oligomerization processes can also take place,^{44,45} which can result in slight distortions of phenylalkyne NMR signals and a yellowing of the initially transparent substrate solution. In our experiments in the cases of phenylacetylene and 3-phenyl-1-propyne, catalysts Pd/TiO₂ and Rh/TiO₂ were found to favor oligomerization (see SI for details, Table S1); however in the case of 1-phenyl-1-propyne, oligomerization was not observed (most likely due to the steric hindrance).

The tested catalysts also showed different selectivities in terms of the formation of specific products. It was found that the most selective catalyst for semihydrogenation of alkynes (to form olefinic moieties) is Pd/TiO₂. Indeed, when this catalyst was used for hydrogenation of phenylacetylene, in the NMR spectra of hydrogenation products (Figure 3) signals from ethylbenzene were practically invisible—an effect that cannot be explained by a low conversion rate (in fact, phenylacetylene hydrogenation conversion over Pd/TiO₂ was higher than that over Rh/TiO₂ (23 wt%), Pt/TiO₂, and Ir/TiO₂, and yet in the spectrum acquired during hydrogenation over the palladium catalyst, ethylbenzene signals have much lower intensities).

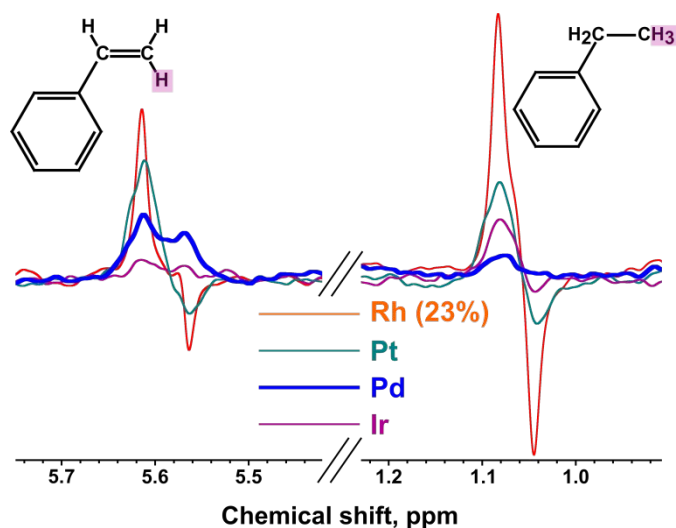


Figure 3- Selected regions of ¹H NMR spectra acquired during phenylacetylene hydrogenation with parahydrogen over Rh/TiO₂ (23 wt%), Pt/TiO₂, Pd/TiO₂, and Ir/TiO₂ catalysts. Note that the signal from protons in the –CH₃ group of ethylbenzene (right region of the spectra) has lower intensity in the spectrum acquired during hydrogenation over palladium catalyst. These spectra are the selected enlarged areas containing the signals of interest, extracted from the spectra shown in Figure 1.

The found selectivity values in 1-phenyl-1-propyne and 3-phenyl-1-propyne hydrogenation are presented in SI (table S2).

Furthermore, the Pd/TiO₂ catalyst demonstrated the highest selectivity for *syn* pairwise addition of the hydrogen to the triple bond. From the same spectrum for this catalyst (Figure 1; a selected enlarged region of the spectra with styrene signals is presented in Figure S9) it can be seen that signal intensity for the proton #4 (originated from *anti* addition of hydrogen) is significantly lower than the intensity of the protons #2 and #3; furthermore, there is little polarization there, indicating that hydrogenation over the palladium catalyst occurs mainly via the *syn* parahydrogen addition route. Nevertheless, relatively low conversion rates and signal enhancements restrict possible application of Pd/TiO₂ catalysts for production of hyperpolarized products in the liquid phase. The kinetics for both pairwise and nonpairwise hydrogen addition were measured (see SI for details).

Conclusions

In this paper liquid-phase hydrogenation of different prototypical phenylalkynes (phenylacetylene, 1-phenyl-1-propyne, and 3-phenyl-1-propyne) over various nanoscale metal catalysts supported on TiO₂ was studied using NMR and parahydrogen-induced polarization. It was demonstrated that the most selective catalyst for alkynes semihydrogenation is Pd/TiO₂; however, for production of hyperpolarized products the most optimal catalyst that provides reasonable values of both conversion and signal enhancement is 4 wt% Rh/TiO₂. Kinetics experiments indicated a similar nature of catalytically active sites for both pairwise and non-pairwise addition routes, given that the experimentally determined reaction orders with respect to hydrogen were close to unity in all cases. This finding is important in the context of potential future studies of these reactions on a larger scale and potentially on industrial scale, because parahydrogen-induced polarization can provide a sensitive readout to investigate the kinetics, selectivity, nature of catalytically active sites, etc.

Conflicts of interest

There are no conflicts to declare.

Acknowledgements

ITC team thanks RFBR (grants 18-43-543023 and 18-33-20019) for the support of catalysts testing in selective hydrogenation reaction with parahydrogen, and the Russian Ministry of Science and Higher Education (AAAA-A16-116121510087-5) for the use of NMR equipment. LMK and IVK thank RSF (grant 19-13-00172) for the support of catalysts synthesis. The US team thanks the NSF for funding support: CHE-1416432, CHE-1416432 and CHE-1836308. We also thank Jamil Mashni for helpful discussions.

Notes and references

- 1 T. Maegawa, A. Akashi, K. Yaguchi, Y. Iwasaki, M. Shigetsura, Y. Monguchi and H. Sajiki, *Chem. Eur. J.*, 2009, **15**, 6953–6963.
- 2 L. E. Oi, M.-Y. Choo, H. V. Lee, H. C. Ong, S. B. A. Hamid and J. C. Juan, *RSC Adv.*, 2016, **6**, 108741–108754.
- 3 A. Elhage, A. E. Lanterna and J. C. Scaiano, *ACS Catal.*, 2017, **7**, 250–255.
- 4 X. Yang, Y. Mueannngern, Q. A. Baker and L. R. Baker, *Catal. Sci. Technol.*, 2016, **6**, 6824–6835.
- 5 A. Yu. Stakheev, P. Markov, A. S. Taranenkov, G. Bragina, G. N. Baeva, O. Tkachenko, I. Mashkovsky and A. Kashin, *Kinetics and Catalysis*, 2015, **56**, 733–740.
- 6 Q. Yuan, D. Zhang, L. van Haandel, F. Ye, T. Xue, E. J. M. Hensen and Y. Guan, *J. Mol. Catal. A Chem.*, 2015, **406**, 58–64.
- 7 S. D. Jackson and L. A. Shaw, *Appl. Catal. A Gen.*, 1996, **134**, 91–99.
- 8 N. Semagina, A. Renken and L. Kiwi-Minsker, *Chem. Eng. Sci.*, 2007, **62**, 5344–5348.
- 9 D. A. Liprandi, E. A. Cagnola, M. E. Quiroga and P. C. L'Argentière, *Catal. Letters*, 2009, **128**, 423–433.
- 10 C. R. Lederhos, P. C. L'Argentière and N. S. Figoli, *Ind. Eng. Chem. Res.*, 2005, **44**, 1752–1756.
- 11 H. Yoshida, T. Zama, S. Fujita, J. Panpranot and M. Arai, *RSC Adv.*, 2014, **4**, 24922–24928.
- 12 C. J. Elsevier, *J. Mol. Catal.*, 1994, **92**, 285–297.
- 13 D. C. Roe, P. M. Kating, P. J. Krusic and B. E. Smart, *Top. Catal.*, 1998, **5**, 133–147.
- 14 J. Bargon, R. Giernoth, L. Greiner, L. Kuhn and S. Laue, *In situ NMR Methods in Catalysis*, Springer, Heidelberg, 2007, vol. 276.
- 15 M. Hunger and W. Wang, *Adv. Catal.*, 2006, **50**, 149–225.
- 16 K. V. Kovtunov, E. V. Pokochueva, O. G. Salnikov, S. F. Cousin, D. Kurzbach, B. Vuichoud, S. Jannin, E. Y. Chekmenev, B. M. Goodson, D. A. Barskiy and I. V. Koptug, *Chem. - An Asian J.*, 2018, **13**, 1857–1871.
- 17 J. B. Hövener, A. N. Pravdivtsev, B. Kidd, C. R. Bowers, S. Glöggler, K. V. Kovtunov, M. Plaumann, R. Katz-Brull, K. Buckenmaier, A. Jerschow, F. Reineri, T. Theis, R. V. Shchepin, S. Wagner, P. Bhattacharya, N. M. Zacharias and E. Y. Chekmenev, *Angew. Chemie - Int. Ed.*, 2018, **57**, 11140–11162.
- 18 K. V. Kovtunov, V. V. Zhivonitko, I. V. Skovpin, D. A. Barskiy and I. V. Koptug, *Top. Curr. Chem.*, 2013, **338**, 123–180.
- 19 T. C. Eisenschmid, R. U. Kirss, P. P. Deutsch, S. I. Hommeltoft, R. Eisenberg, J. Bargon, R. G. Lawler and A. L. Balch, *J. Am. Chem. Soc.*, 1987, **109**, 8089–8091.
- 20 C. R. Bowers and D. P. Weitekamp, *Phys. Rev. Lett.*, 1986, **57**, 2645–2648.
- 21 C. R. Bowers and D. P. Weitekamp, *J. Am. Chem. Soc.*, 1987, **109**, 5541–5542.
- 22 S. A. Colebrooke, S. B. Duckett, J. A. B. Lohman and R. Eisenberg, *Chem. Eur. J.*, 2004, **10**, 2459–2474.
- 23 A. S. Kiryutin, G. Sauer, A. V. Yurkovskaya, H. H. Limbach, K. L. Ivanov and G. Buntkowsky, *J. Phys. Chem. C*, 2017, **121**, 9879–9888.
- 24 O. G. Salnikov, H.-J. Liu, A. Fedorov, D. B. Burueva, K. V. Kovtunov, C. Co Eret and I. V. Koptug, *Chem. Sci.*, 2017, **8**, 2426–2430.
- 25 L. S. Bouchard, K. V. Kovtunov, S. R. Burt, S. Anwar, I. V. Koptug, R. Z. Sagdeev and A. Pines, *Angew. Chemie - Int. Ed.*, 2007, **46**, 4064–4068.
- 26 L.-S. S. Bouchard, S. R. Burt, M. S. Anwar, K. V. Kovtunov, I. V. Koptug and A. Pines, *Science*, 2008, **319**, 442–445.
- 27 E. W. Zhao, H. Zheng, K. Ludden, Y. Xin, H. E. Hagelin-Weaver and C. R. Bowers, *ACS Catal.*, 2016, **6**, 974–978.
- 28 E. W. Zhao, H. Zheng, R. Zhou, H. E. Hagelin-Weaver and C. R. Bowers, *Angew. Chemie - Int. Ed.*, 2015, **54**, 14270–14275.
- 29 A. M. Balu, S. B. Duckett and R. Luque, *Dalt. Trans.*, 2009, 5074–5076.
- 30 I. V. Koptug, V. V. Zhivonitko and K. V. Kovtunov, *ChemPhysChem*, 2010, **11**, 3086–3088.
- 31 K. V. Kovtunov, D. A. Barskiy, O. G. Salnikov, R. V. Shchepin, A. M. Coffey, L. M. Kovtunova, V. I. Bukhtiyarov, I. V. Koptug and E. Y. Chekmenev, *RSC Adv.*, 2016, **6**, 69728–69732.
- 32 S. Glöggler, A. M. Grunfeld, Y. N. Ertas, J. McCormick, S. Wagner, P. P. M. Schleker and L. Bouchard, *Angew. Chemie Int. Ed.*, 2015, **54**, 2452–2456.
- 33 L. B. Bales, K. V. Kovtunov, D. A. Barskiy, R. V. Shchepin, A. M. Coffey, L. M. Kovtunova, A. V. Bukhtiyarov, M. A. Feldman, V. I. Bukhtiyarov, E. Y. Chekmenev, I. V. Koptug and B. M. Goodson, *J. Phys. Chem. C*, 2017, **121**, 15304–15309.
- 34 J. McCormick, S. Korchak, S. Mamone, Y. N. Ertas, Z. Liu, L. Verlinsky, S. Wagner, S. Glöggler and L. S. Bouchard, *Angew. Chemie - Int. Ed.*, 2018, **57**, 10692–10696.
- 35 K. V. Kovtunov, D. A. Barskiy, R. V. Shchepin, O. G. Salnikov, I. P. Prosvirin, A. V. Bukhtiyarov, L. M. Kovtunova, V. I. Bukhtiyarov, I. V. Koptug and E. Y. Chekmenev, *Chem. Eur. J.*, 2016, **22**, 16446–16449.
- 36 S. B. Duckett and N. J. Wood, *Coord. Chem. Rev.*, 2008, **252**, 2278–2291.
- 37 I. V. Koptug, K. V. Kovtunov, S. R. Burt, M. Sabieh Anwar, C. Hilty, S.-I. Han, A. Pines and R. Z. Sagdeev, *J. Am. Chem. Soc.*, 2007, **129**, 5580–5586.
- 38 T. Ratajczyk, T. Gutmann, P. Bernatowicz, G. Buntkowsky, J. Frydel and B. Fedorczyk, *Chem. Eur. J.*, 2015, **21**, 12616–12619.
- 39 I. V. Skovpin, V. V. Zhivonitko and I. V. Koptug, *Appl. Magn. Reson.*, 2011, **41**, 393–410.
- 40 I. V. Skovpin, V. V. Zhivonitko, R. Kaptein and I. V. Koptug, *Appl. Magn. Reson.*, 2013, **44**, 289–300.
- 41 A. Corma, O. G. Salnikov, D. A. Barskiy, K. V. Kovtunov and I. V. Koptug, *Chem. Eur. J.*, 2015, **21**, 7012–7015.
- 42 I. V. Skovpin, V. V. Zhivonitko, I. P. Prosvirin, D. F. Khabibulin and I. V. Koptug, *Zeitschrift für Phys. Chemie*, 2017, **231**, 575–592.
- 43 E. W. Zhao, R. Maligal-Ganesh, C. Xiao, T. Goh, Z. Qi, Y. Pei, H. E. Hagelin-Weaver, W. Huang and C. R. Bowers, *Angew. Chemie*, 2017, **129**, 3983–3987.
- 44 O. G. Salnikov, K. V. Kovtunov and I. V. Koptug, *Sci. Rep.*, 2015, **5**, 13930.
- 45 V. V. Zhivonitko, I. V. Skovpin, M. Crespo-Quesada, L. Kiwi-Minsker and I. V. Koptug, *J. Phys. Chem. C*, 2016, **120**, 4945–4953.

